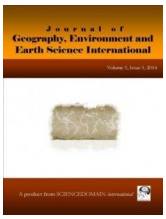

Journal of Geography, Environment and Earth Science International
8(1): 1-18, 2016; Article no.JGEESI.28198
ISSN: 2454-7352

SCIENCEDOMAIN *international*
www.sciencedomain.org

Geochemistry and Petrogenesis of Mafic Doleritic Dykes at Mbaoussi (Adamawa Plateau, Cameroon, Central Africa)

O. F. Nkouandou[1], J. M. Bardintzeff[2*], P. Dourwe Dogsaye[1] and A. Fagny Mefire[1]

[1]Faculty of Science, University of Ngaoundéré, P.O.Box 454, Ngaoundéré, Cameroon.
[2]Univ. Paris-Sud, Sciences de la Terre, Volcanologie, Planétologie, UMR CNRS 8148 GEOPS, Bât. 504, Université Paris-Saclay, F-91405 Orsay, France.

Authors' contributions

This work was carried out in collaboration between all authors. Authors OFN, PDD and AFM made field work. Author OFN designed the study, wrote the protocol and wrote the first draft of the manuscript. Authors OFN and JMB managed the literature searches and the selections of samples for analyses. Author JMB wrote the final version of the manuscript. All authors read and approved the final manuscript.

Article Information

DOI: 10.9734/JGEESI/2016/28198
Editor(s):
(1) Zeyuan Qiu, Department of Chemistry and Environmental Sciences, New Jersey Institute of Technology, USA.
(2) Ioannis K. Oikonomopoulos, Core Laboratories LP., Petroleum Services Division, Houston Texas, USA.
(3) Anthony R. Lupo, Department of Soil, Environmental, and Atmospheric Science, University of Missouri, Columbia, USA.
Reviewers:
(1) I. V. Haruna, Modibbo Adama University of Technology, Yola, Nigeria.
(2) Kouankap N. G. Djibril, HTTC, University of Bamenda, Cameroon.
(3) Sarjesh Laishram, Geological Survey of India, India.
Complete Peer review History: http://www.sciencedomain.org/review-history/16647

Original Research Article

Received 7th July 2016
Accepted 17th October 2016
Published 25th October 2016

ABSTRACT

Giant mafic doleritic dyke swarms crosscut the Mbaoussi granitoid basement to the North of Ngaoundéré, in Adamawa plateau (Cameroon, Central Africa). The dyke swarm orientation might correspond to reworked Late Pan-African fault zones. Mbaoussi doleritic dykes display intergranular to ophitic and sub-ophitic textures and are mainly composed of clinopyroxene, plagioclase feldspar and Fe-Ti oxides. ICP-MS and ICP-AES geochemical data show both slight alkaline affinities according to total alkalis-silica contents and continental tholeiitic signature evidenced by Nb-, Ta-

**Corresponding author: E-mail: jacques-marie.bardintzeff@u-psud.fr;*

and Ti-depletions. Primary magmas suffered fractional crystallization coupled with assimilation of continental materials, to produce a sub-alkali basalt to trachybasalt to basaltic trachyandesite lava series. Low values (3-7) of $(Ce/Yb)_N$ suggest fairly high partial melting degree of the source. This source was probably the sub-continental lithospheric mantle, whose composition was close to fertile mantle component, yet Nb-Ta depleted after a former subduction.

Keywords: Dyke; dolerite; continental tholeiite; Mbaoussi; Adamawa plateau; Cameroon; Central Africa.

1. INTRODUCTION

The Adamawa continental crust, in North-East Cameroon, is part of the Central Pan-African Fold Belt (CPFB) (Fig. 1) It is dissected by numerous Pan-African N00° N30°E, N50°E, N70°E, N90°E and N160°E strike slip-faults [1], probably down to the mantle [2]. Geophysical studies on the Adamawa horst [3,4,5,6,7,8,9] have shown up to 1 km-high Tertiary uplift relative to its vicinity [9,10], due to upward migration of the lithosphere-asthenosphere boundary [11]. Mesozoic and Cenozoic rejuvenation of Pan-African Adamawa faults [1] fostered probably Mio-Pliocene volcanism [12,13] of the Adamawa plateau. Doleritic dyke swarms located near Biden, 5 km South-East of Ngaoundéré [14], Likok, 70 km South-East of Ngaoundéré [15], and Mbaoussi, 40 km North-East of Ngaoundéré (this study) are linked to one or multiple tectonic manifestations which have affected the Central African continental crust. These tectonic events can be associated to (i) reactivation of the Pan-African crust [16]: The dyke swarm orientation might result from reworked Late Pan-African fault network affecting the granitoid basement of Adamawa plateau [1], during multiple episodes in Ordovician (c. 450 Ma) and Jurassic times, (ii) Late Jurassic-Early Cretaceous opening of the South Atlantic Ocean [17], (iii) development of North Cameroon Djerem and Mbere Cretaceous basins [18] and/or (iv) development of West and Central African Rift Systems [5].

In this paper, we present a newly discovered doleritic dyke swarm near Mbaoussi, in Adamawa plateau (Fig. 1). From field-works and chemical analyses, and by comparison with nearby fairly similar dykes, hypotheses on their petrogenesis are offered.

2. GEOLOGICAL SETTING

Adamawa plateau is part of the Adamawa-Yadé Domain (AYD), a Paleoproterozoic basement dismembered during Pan-African orogeny. It is bounded by two other Paleoproterozoic basements, the West Cameroon Domain (WCD) to the north-west, and the Yaoundé Domain (YD) to the south-east (Fig. 1B, [19]). Adamawa-Yadé Domain is a terrane within the Central Pan-African Fold Belt (CPFB) which had a long and complex crustal evolution with strong imprint of Neoproterozoic events [19].

Ngaoundéré Pan-African granitoids [20] are made up of 615 to 575 ± 27 Ma granites crosscutting a ca. 2.1 Ga remobilized basement composed of meta-sedimentary and meta-igneous rocks that had underwent medium- to high-grade Pan-African metamorphism. All granitoids are enriched in Large Ion Lithophile Elements (LILE) relative to High Field Strength Elements (HFSE) and display negative Nb-Ta and Ti anomalies. They evidence a high-K calc-alkaline suite with I-type signature, as defined by [21]. They may derive from differentiation of mafic magma issued from enriched subcontinental lithospheric mantle with possible crustal assimilation.

The thickness of lithosphere beneath Adamawa plateau is reduced to 80 km, whereas continental crust is 20 km-thick above an anomalous low-density asthenosphere, as deduced from gravity (negative Bouguer anomalies, [7]) and seismic data [22]. The basement is intensely dissected by Pan-African faults: according to [1], some faults (N70°E) were reworked during Albian-Aptian times. Previous studies on dyke swarms in Adamawa plateau suggest identified doleritic dykes of continental tholeiite composition [14] associated with post-Pan-African extensional magmatism [15]. The chemical features of these rocks have been interpreted as fingerprints of a sub-continental lithospheric source mantle sharing E-MORB components which may have been contaminated during a former subduction event. The present study concerns large dolerite dyke swarm discovered near Mbaoussi.

3. MATERIALS AND METHODS

Petrographic observations were carried out on 20 thin sections prepared from representative samples of the dyke swarms at Geosciences (GEOPS) Laboratory, University Paris-Sud Orsay, France. Major and trace element analyses were determined for 10 representative samples by ICP-AES and ICP-MS at the Acme Laboratory, Vancouver, Canada. Prepared samples are mixed with $LiBO_2/Li_2B_4O_7$ flux. The samples were dissolved in a Teflon pressure bomb, using a 1:1 mixture of HF and $HClO_4$ at 180°C, and then taken up in an HNO_3 solution with an In-Re international standard. After dissolution in HF-$HClO_4$, the samples were taken up in a mixture of HNO_3, HCl and HF and diluted. These solutions were measured within 24 hours after dilution to prevent absorption of HFSE.

Loss on ignition (LOI) was determined by igniting a sample split at 1000°C and then measuring the weight loss.

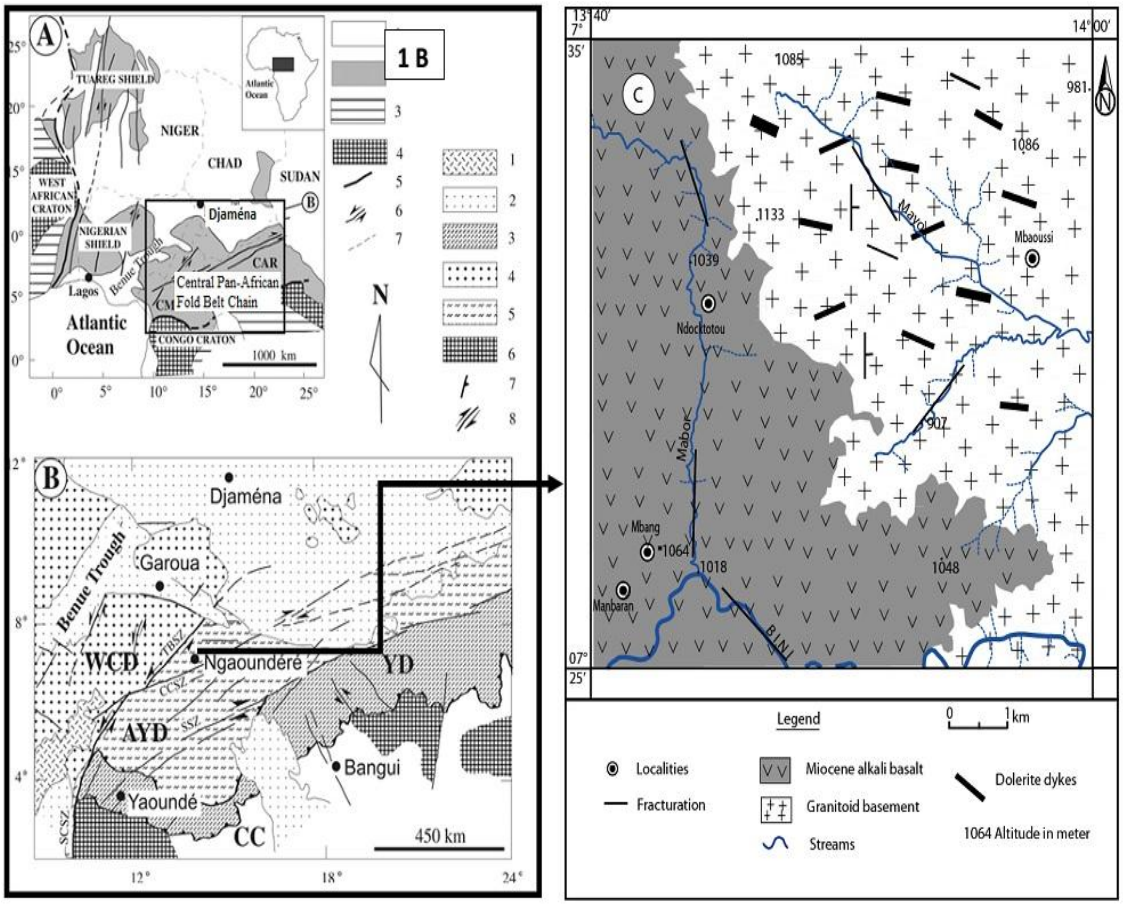

Fig. 1. (A) Geological map from [19] showing the location of Fig.1B. 1: Post-Pan-African cover; 2: Pan-African belt; 3: Pre-Mesozoic platform series; 4: Archean to Paleoproterozoic cratons; 5: Craton limits; 6: Faults; 7: State boundaries. CAR: Central African Republic; CM: Cameroon. (B) Enlarged map of the Pan-African belt north of the Congo craton; 1: Cenozoic volcanic rocks of the Cameroon line; 2: Mesozoic sediments; 3: Yaoundé Domain (YD); 4: Western Cameroon Domain (WCD); 5: Adamawa-Yadé Domain (AYD); 6: Congo craton (CC); 7: Thrusts; 8: Strike slip faults: TBSZ: Tcholliré-Banyo shear zone; CCSZ: Central Cameroon shear zone; SSZ: Sanaga shear zone; SCSZ: Southwest Cameroon shear zone. (C) Mbaoussi geological map showing dykes in the granitoid basement overlain by Miocene basaltic lavas. Main fracturations and streams are indicated

4. RESULTS

4.1 Dyke Swarm

The Mbaoussi dyke swarm crosscut the Pan-African granitic basement, throughout a 8 x 6 km area (Figs. 1, 2). 43 dykes have been identified, 10 of them have been analyzed. Individual dykes range in scale from 3 to 34 m in width. Their major trend is orientated N100°-130° and the N70°-80° trend is minor (Fig. 3), both being parallel to Pan-African regional lineaments [1] [18]. As observed in hand specimen, crystal sizes increase from margin to core.

4.2 Petrography

In hand specimen, samples are light to dark grey and coated with 2 mm to 2 cm-thick light brown patina. All samples exhibit a coarse grained texture with crystals of whitish feldspar (from 0.4 x 1.0 cm to 1.6 x 3.2 cm and 10 to 20 volume %), black crystals of pyroxene or oxides (0.2 to 0.4 mm, 5 volume %), rectangular or square shaped golden crystals (pyrite group? 3 volume %) in the matrix. Hydrothermal alteration is shown by green epidote crystals, while clay mineral and pockets of carbonate evidence weathering. Centimetre-large xenoliths of basement granite occur in some dykes.

(A) (B)

Fig. 2. View (A) and measurement of width (B) of a dyke outcrop. Dyke margins are highlighted with dashed lines

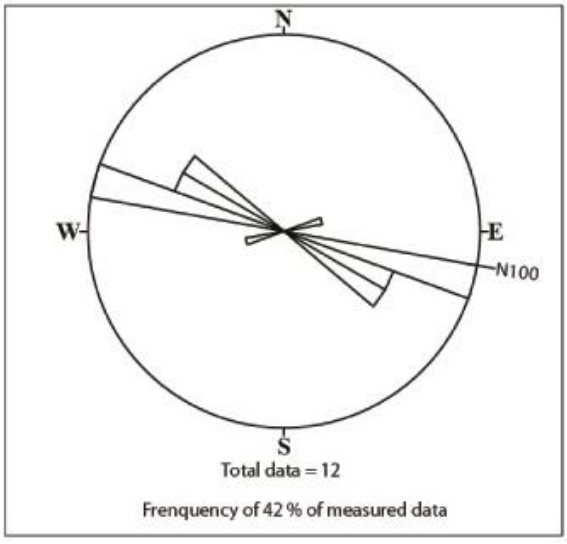

Fig. 3. Rose diagram representing main orientations of Mbaoussi dykes (total data = 12, 5 of them (42 %) follow the N100°-110° direction)

Under microscope, dolerites of Mbaoussi exhibit classic ophitic, sub-ophitic or doleritic textures (Fig. 4A, 4B and 4C, respectively). They are composed of elongate plagioclase crystals partially enclosed in clinopyroxene crystals. Plagioclase sometimes displays speckled and resorption cores that could present sieve-textures (Fig. 4A). Clinopyroxene phenocrysts are subhedral and brown or pinkish in colour, indicating that they are Ti-rich. Some clinopyroxene phenocrysts show skeleton features and sometimes intergrowths with plagioclase crystals as intersertal dolerite textures. They are frequently associated with anhedral oxide phenocrysts and can be converted into green patches by alteration. Two populations of Fe-Ti oxides were observed: (1) subhedral primary phenocrysts, commonly enclosed in clinopyroxene and plagioclase, correspond to the earliest crystallized mineral phase, (ii) skeletal oxide crystals result from pyroxene alteration.

4.3 Geochemistry

Major and trace element compositions of Mbaoussi dolerite dyke selected samples are listed in Table 1. Because there are distinct variation ranges in some elements (Si, Mg, Ti, K, and some others) samples are classified into two groups, based on Mg number (atomic Mg# = 100*(MgO/40.32)/(MgO/40.32+FeOt/71,85)), following [23] definition. Mafic or primitive (SiO_2 contents between 44.9 and 47.5 wt%) group I dolerites have Mg# ≥ 44 (up to 58). More felsic (SiO_2 contents between 49.7 and 53.0 wt%) group II dolerites have Mg# ≤ 44. The two groups are well discriminated in the IUGS (Na_2O+K_2O) vs. SiO_2 diagram [24] (Fig. 5). Group I dolerites are basalts and trachybasalts, whereas group II dolerites are trachybasalts and basaltic trachyandesites. In both groups, LOI range is about 3 wt%.

Both groups show slightly alkaline affinities according to alkali / silica contents, using [25] boundary (Fig. 5). In the TiO_2 vs. Y/Nb diagram of [26], constant Y/Nb ratios of nearly 2 evidenced a continental tholeiitic signature (Fig. 6). Nb-, Ta- and Ti-depletions characterize the two groups of dolerites.

CIPW normative calculations distinguish two low nepheline normative compositions (in group I), three quartz normative compositions (in group II), and five (within both groups I and II) hypersthene and olivine normative (silica saturated) compositions (Table 1). With increasing SiO_2 contents, CIPW normative compositions shift progressively from silica undersaturated to saturated to oversaturated.

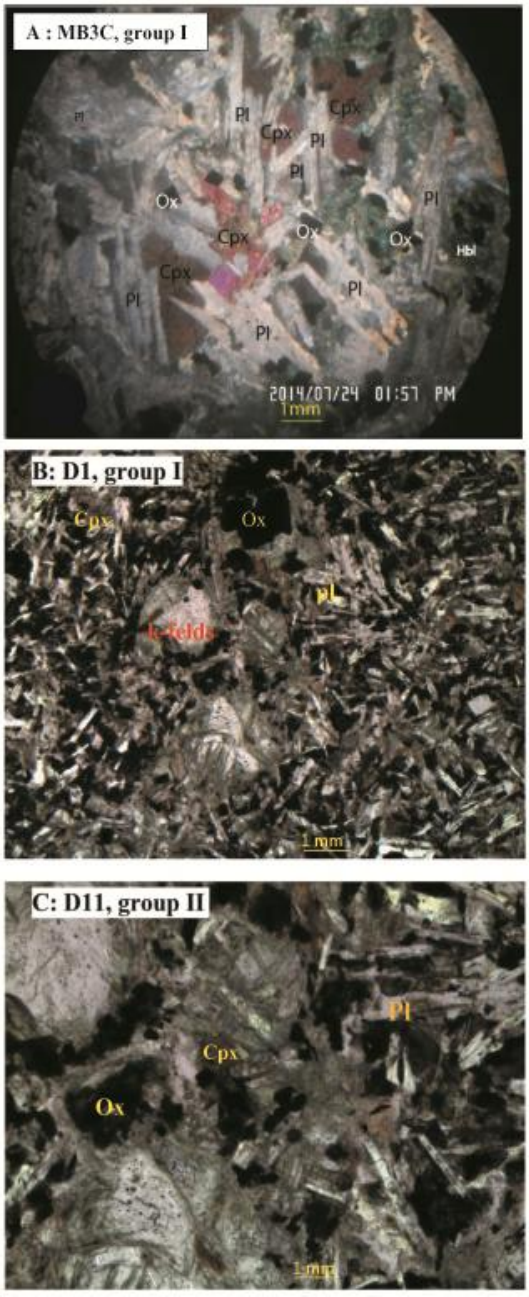

Fig. 4. Elongate plagioclase and anhedral oxide crystals with pyroxene phenocrysts in ophitic (A) and sub-ophitic or intersertal (B and C) doleritic texture. Magnification x 2. XPL. Cpx = clinopyroxene, Hbl = hornblende, Ox = Fe-Ti oxide, Pl = plagioclase

Table 1. Major and trace element analyses and CIPW normative compositions of Mbaoussi dolerite dyke swarm. Cr has been analyzed as Cr_2O_3 (presented with 3 significant digits), except for MB3C in which Cr contents have been calculated in ppm. Total iron as FeO. LOI presented with one significant digit

Dyke	Group I						Group II			
Sample	D10	D14	D11	MB3C	D2	D12	D13	D16	D1	D15
SiO_2 wt%	44.90	45.82	46.31	47.16	47.51	49.68	50.07	51.39	51.98	53.01
TiO_2	2.22	2.91	1.82	1.51	1.73	2.21	2.11	2.43	2.48	2.28
Cr_2O_3	0.009	0.006	0.019		0.020	0.004	0.006	0.004	0.004	0.004
Al_2O_3	16.13	15.44	16.61	16.58	16.58	15.65	15.16	14.64	14.24	14.72
FeOt	12.79	12.95	10.90	10.47	11.65	11.38	12.62	12.78	12.78	11.70
MnO	0.18	0.19	0.16	0.17	0.17	0.17	0.19	0.18	0.18	0.17
MgO	6.37	5.72	7.41	8.16	6.52	4.95	4.58	3.72	3.53	3.29
CaO	8.05	7.54	9.33	9.06	8.86	6.39	6.62	5.47	5.88	5.74
Na_2O	3.06	3.17	2.85	2.99	2.65	3.64	2.64	2.75	2.90	2.83
K_2O	1.90	2.30	0.97	0.96	0.64	2.22	2.83	3.02	2.32	2.94
P_2O_5	0.47	0.53	0.32	0.24	0.38	0.45	0.45	0.52	0.55	0.50
LOI	3.6	3.0	3.0	3.54	3.0	2.9	2.4	2.7	2.8	2.5
Sum	99.68	99.58	99.70	100.86	99.71	99.64	99.68	99.60	99.64	99.68
Quartz	0.00	0.00	0.00	0.00	0.00	0.00	0.00	2.90	5.15	5.22
Corundum	0.00	0.00	0.00	0.00	0.00	0.00	0.00	0.00	0.00	0.00
Orthoclase	11.23	13.59	5.73	5.69	3.78	13.12	16.72	17.85	13.71	17.37
Albite	19.96	22.57	24.12	25.33	22.42	30.80	22.34	23.27	24.54	23.95
Anorthite	24.66	21.11	29.66	28.96	31.45	19.81	21.16	18.68	18.99	18.78
Leucite	0.00	0.00	0.00	0.00	0.00	0.00	0.00	0.00	0.00	0.00
Nepheline	3.22	2.30	0.00	0.00	0.00	0.00	0.00	0.00	0.00	0.00
Diopside	10.06	10.59	11.86	11.75	8.23	7.41	7.29	4.24	5.54	5.40
Wollastonite	0.00	0.00	0.00	0.00	0.00	0.00	0.00	0.00	0.00	0.00
Hypersthene	0.00	0.00	0.82	0.18	18.47	7.98	20.43	20.81	19.60	17.92
Olivine	18.31	16.28	17.45	19.25	5.13	9.42	0.99	0.00	0.00	0.00
Magnetite	2.21	2.23	1.88	1.81	2.01	1.96	2.18	2.20	2.20	2.02
Ilmenite	4.22	5.53	3.46	2.87	3.29	4.20	4.01	4.62	4.71	4.33
Haematite	0.00	0.00	0.00	0.00	0.00	0.00	0.00	0.00	0.00	0.00
Apatite	1.09	1.23	0.74	0.56	0.88	1.04	1.04	1.20	1.27	1.16
Mg#	47.02	44.04	54.78	58.14	49.93	43.67	39.27	34.15	32.99	33.38
Be (ppm)	2	<1	3	0.861	<1	2	<1	2	4	2
Rb	73.8	67.1	20.1	40.16	21.1	75.7	83.1	138.0	85.2	91.3
Sr	652.1	691.8	506.1	531.3	506.1	594.8	521.3	765.4	614.1	518.8
Cs	0.4	0.7	1.1	0.698	1.2	0.3	0.2	0.4	0.3	0.5
Ba	544	787	238	367.5	370	570	716	1049	946	907
V	200	233	204	180	179	167	144	199	201	186
Cr	62	41	130	194.6	137	27	41	27	27	27
Co	39.1	38.4	38.8	44.45	40.4	34.2	31.0	29.9	29.2	28.1
Ni	50	35	65	76.1	99	35	21	20	24	24
Cu	31.2	25.7	38.6	37.93	47.7	23.6	21.2	20.0	25.1	15.6
Y	30.5	38.5	26.5	22.72	29.3	36.5	37.5	49.2	49.0	46.4
Zr	235.9	301.1	194.7	129.4	218.9	345.4	300.0	352.9	367.9	348.2
Nb	14.5	19.8	11.6	8.779	11.4	20.2	16.8	20.1	20.9	19.7
Hf	5.4	6.5	4.2	3.14	5.4	7.4	6.7	8.1	8.4	8.2
Ta	0.8	1.2	0.8	0.652	0.8	1.1	1.2	1.2	1.1	1.3
Th	1.4	2.0	1.6	0.95	2.3	6.8	4.4	4.0	5.0	5.4
U	0.4	0.4	0.3	0.223	0.3	0.9	0.8	0.6	0.8	0.8
La	24.5	31.7	17.5	11.57	26.1	43.0	37.3	45.1	48.6	46.8
Ce	60.9	75.5	42.9	27.84	55.7	94.0	82.8	102.7	108.8	103.2

Dyke	Group I					Group II				
Pr	7.32	9.23	5.40	3.752	7.27	11.11	9.79	11.65	12.72	12.04
Nd	30.3	40.8	23.1	16.53	31.4	43.0	40.8	51.3	52.5	49.6
Sm	6.89	8.04	5.22	4.059	6.13	9.29	8.45	9.86	11.12	10.05
Eu	2.14	2.59	1.66	1.497	1.84	2.19	2.33	2.91	2.84	2.90
Gd	6.75	8.41	5.57	4.008	6.15	8.24	8.67	10.72	11.09	9.84
Tb	1.05	1.26	0.86	0.65	1.00	1.26	1.30	1.59	1.65	1.57
Dy	5.81	7.05	5.10	4.139	5.44	6.77	7.14	8.82	9.25	8.54
Ho	1.18	1.43	0.98	0.881	1.13	1.37	1.49	1.89	1.90	1.81
Er	3.35	3.83	2.78	2.318	3.15	4.01	4.02	5.07	5.32	5.19
Tm	0.45	0.54	0.41	0.333	0.47	0.54	0.63	0.75	0.77	0.72
Yb	2.78	3.36	2.64	2.239	3.01	3.73	3.75	4.91	5.02	4.41
Lu	0.42	0.49	0.40	0.34	0.45	0.54	0.58	0.67	0.70	0.73
Ga	16.7	17.7	15.7	17.29	16.8	18.4	17.2	20.6	19.4	20.7
Sn	1	2	2	1.606	2	2	2	3	3	3
Sc	24	26	29	30.87	26	20	24	25	25	23
W	<0.5	<0.5	<0.5	< L.D.	<0.5	<0.5	<0.5	<0.5	0.5	0.5
Pb	0.0	0.0	0.0	3.3	0.0	0.0	0.0	0.0	0.0	0.0

In both groups, transitional element compositions display very low contents (e.g. 20-99 ppm Ni, 27-195 ppm Cr, 28-45 ppm Co and 25-48 ppm Cu, correlated with 33-58 Mg#, Table 1). They differ from values corresponding to primitive magmas, with Ni = 250-350 ppm, Cr = 500-600 ppm and Mg# > 67 [27]. The lowest contents in transition elements are found in evolved dolerites of group II.

Alkali and alkaline earth elements (Rb, Ba, Sr) contents are fluctuating from group I to group II. Sr contents are high (500-765 ppm) in Mbaoussi dolerites, compared to Obudu (408 ppm, [28]), Bangangté, Dschang and Manjo (359-413 ppm, [29]) dolerites. Sr contents of Biden continental tholeiites are fairly high (730-793 ppm, [14]). Ba contents are higher in group II (up to 1049 ppm) than in group I, but lower than Biden continental tholeiites (1700-1800 ppm). Rb contents are lower in group I (20-74 ppm) and Obudu (18 ppm) dolerites and higher in group II (75-138 ppm), like Biden tholeiites (156-199 ppm). Rb/Ba and Rb/Sr ratios are low and are respectively 0.08-0.14 and 0.04-0.11 in group I, and 0.9-0.13 and 0.13-0.18 in group II Mbaoussi dolerites.

Incompatible high-field strength trace elements (HFSE) such as Zr, Nb, Ta, Th, Hf and LREE yield increasing contents from group I to group II (Table 1). Zr/Nb (15-19), Nb/Ta (13-19) and Zr/Hf (41-47) ratios are fairly constant. Zr/Nb ratios are close to CHUR (19.57, [30]) and are lower than those of DM and MORB values that range between 26 [30] and 60 [31]. Comparative data of Table 2 show that Zr/Nb ratios yield lower values and wide variations from 8 to 12 in Bangangté, Dschang and Manjo dolerites and quite constant ratio of 14 in Biden dolerites. Nb/U and Ce/Pb ratios are high in group I (36-50 and 17-20, respectively). Sample MB3C of group I differs with a rather low Ce/Pb ratio of 8.6, compared to values of 17-20 in group I and 10-24 in group II. Y contents vary from 23 to 39 ppm in group I and from 36 to 49 ppm in group II. Mbaoussi dolerite compositions fall within both fields of alkali basalts (AI and AII) and tholeiitic basalts (AI, AII and C) in the Zr-Nb-Y diagram (Fig. 9) after [32]. Th/Ta ratios are bracketed between 1.5 and 2.9 in group I and between 3.3 and 6.2 in group II. In Th/Yb vs. Ta/Yb diagram (Fig. 10, after [33]), Mbaoussi dolerites plot within the ocean island arcs field above the enriched mantle.

Primitive mantle-normalized multi-element diagram (values from [34]) shows fractionated patterns with group II above group I (Fig. 11A). Patterns are similar to those of continental tholeiites worldwide. Mbaoussi patterns resemble other dolerites in Cameroon, but differ from alkali basalt (Fig. 11). Group II dolerites are characterized by Rb, K, Ba, Pb and Zr positive anomalies and Nb, Ta, P and Ti negative anomalies.

REE contents (Fig. 11B) show fractionated LREE to HREE patterns, with slightly negative Eu anomaly. Group I $(Ce/Yb)_N$ ratios range from 3.2 to 5.7, and vary from 5.7 to 6.8 in group II. $(Gd/Yb)_N$ and $(La/Sm)_N$ ratios vary respectively between 1.5 and 2.0 and 1.8 and 2.9 in both dolerite groups.

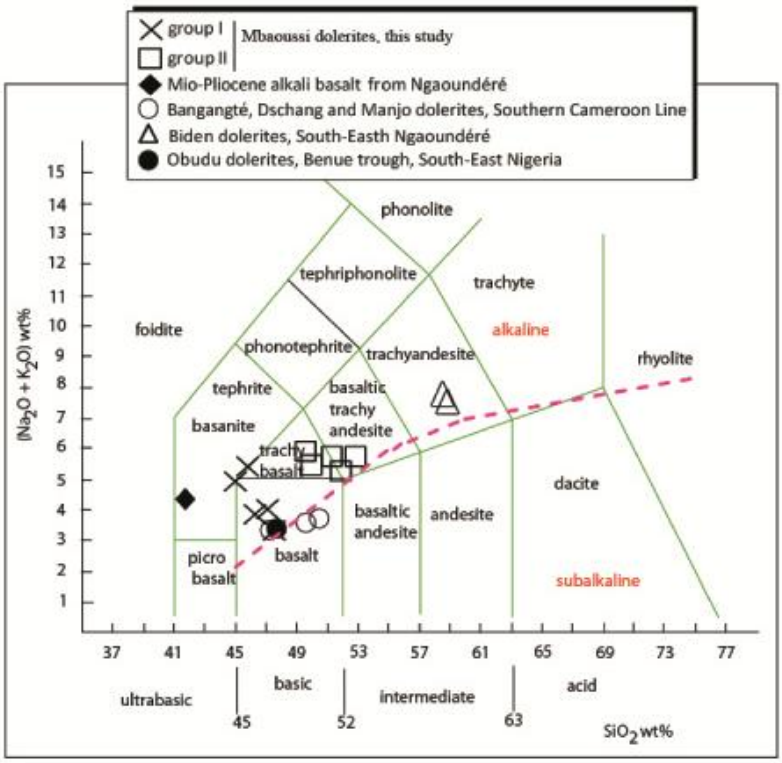

Fig. 5. Total alkalis (Na_2O+K_2O) vs. SiO_2 (wt % volatile-free recalculated compositions, after [24] diagram of representative dolerite dyke of Mbaoussi. Dolerites of Biden [14], Obudu [28], Bangangté, Dschang and Manjo [29] and Mio-Pliocene alkali basalts of Ngaoundéré area [12] are added for comparison. Dashed curve separates alkaline from subalkaline fields, according to [25]

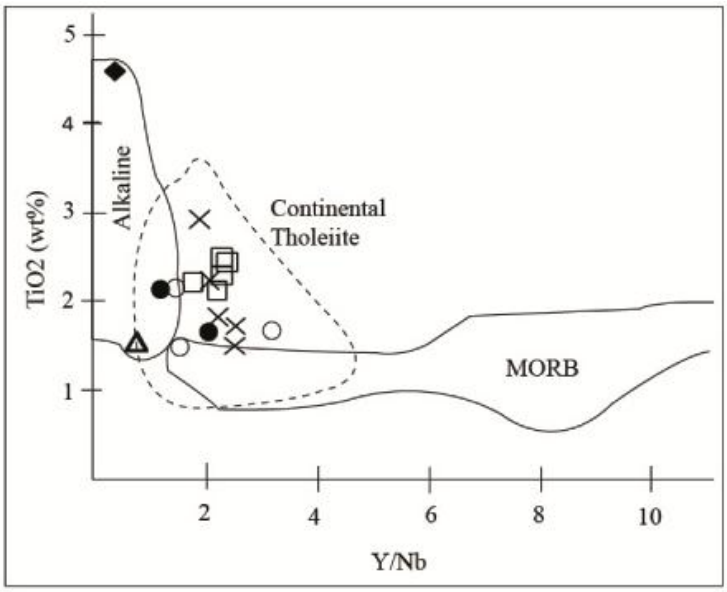

Fig. 6. Mbaoussi dolerite compositions plot in the continental tholeiitic field in TiO_2 vs. Y/Nb discrimination diagram (after [26]). Same symbols as Fig. 5

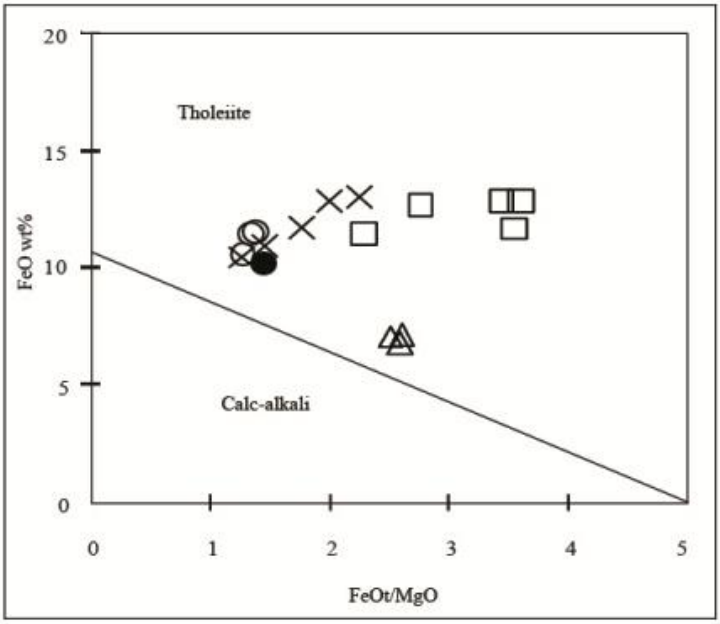

Fig. 7. Mbaoussi dolerites plot in the tholeiitic field in the FeOt vs. FeOt/MgO diagram (after [50]). Same symbols as Fig. 5.

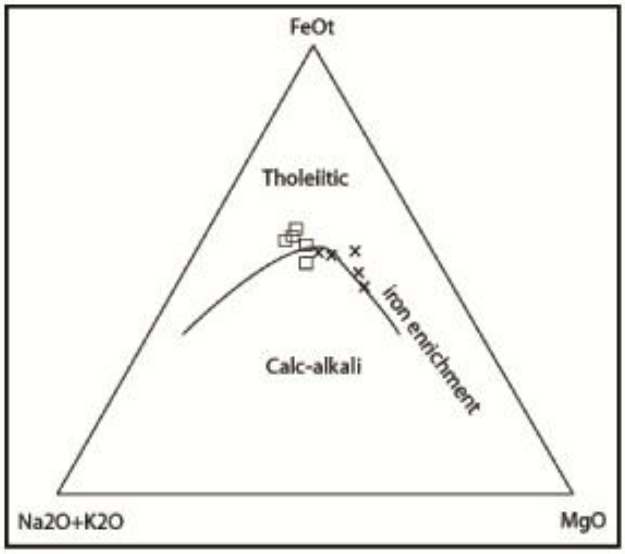

Fig. 8. Alkalis-ΣFeO-MgO diagram with tholeiite and calc-alkaline fields and the dividing line proposed by [51]. Same symbols as Fig. 5

In the Th/Ta vs. La/Yb diagram (after [35]), Mbaoussi dolerites define an array of increasing ratios from FOZO mantle component toward Upper Crust (UC) end-member, with two samples near the Lower Continental Crust (LC) end-member (Fig. 12). La/Ba vs. La/Nb diagram (after [36]) diagram depicts a cluster within the lithospheric quadrangle (Fig. 13). Gd/Yb ratios (1.7-2.5) are higher than in Bangangté, Dschang and Manjo dykes, whereas Biden continental tholeiites display even higher values (6.7-7.3). Such high values indicate a continental tholeiite feature.

Table 2. Comparison of trace-element ratios of Mbaoussi dolerites with other doleritic dykes of Cameroon and mantle sources (see references in the text)

Element ratios	La/Ta	La/Nb	La/Ba	Zr/Nb	La/Yb	Th/Ta	Nb/Th	Th/U	Nb/U	$(Th/La)_N$
Mbaoussi:										
Group I	17-27	1.3-1.7	0.03-07	14.74-19.20	5-9.4	1.5-2.9	5.0-10.4	3.0-7.7	36-50	0.44-0.71
Group II	30-45	2.1-2.4	0.4-0.8	17.10-17.89	9-11	3.3-6.2	3.0-5.0	5.0-7.6	21-34	0.68-1.22
Bagangté	32.75	2.05	0.10	12.0	9.27	2.24	7.14			0.52
Dschang	24.33	1.52	0.05	10.5	11.13	2.20	7.28			0.70
Manjo	15.46	0.94	0.13	8.4	8.50	1.35	11.85			0.67
Biden	52-55	3.4-3.6	0.05	14.0	66-71	7-8	1.99			1.0-1.14
Obudu						0.8				
Continental tholeiite						5.19	3.08	3.42		
NMORB					0.8-2.0	0.5-1.3				
Continental crust									9-12	
PMORB					25±5		19		47±10	

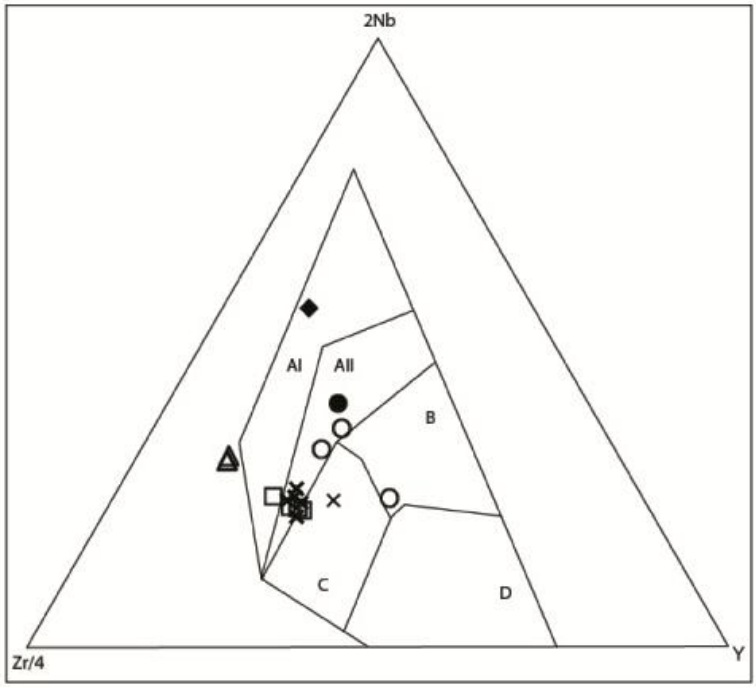

Fig. 9. Zr/4-2Nb-Y diagram (after [32]). AI and AII: Alkali basalts from within-plate environments, AI, AII and C: Tholeiitic basalts from within-plate environments, C and D: Volcanic Arc Basalt (VAB), D: N-type MORB, B: P-type MORB. Data for comparison are indicated. Same symbols as Fig. 5

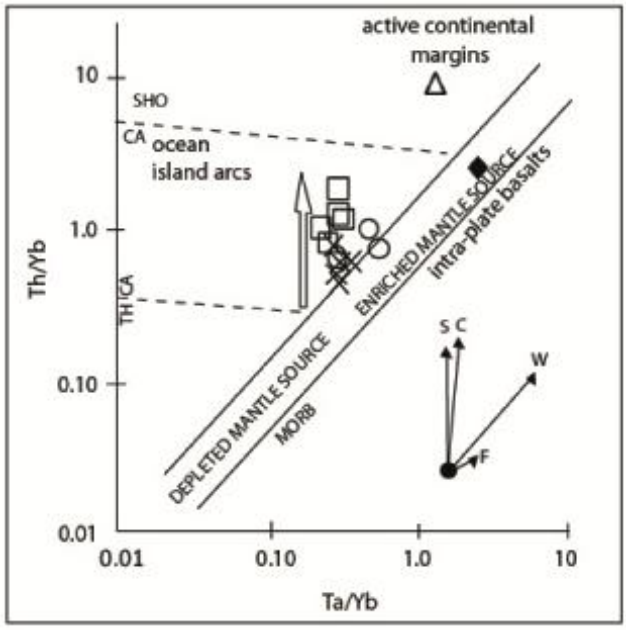

Fig. 10. Th/Yb vs. Ta/Yb diagram (after [33]). Data for comparison and symbols are the same as in Fig. 5. S: enrichment related to subduction zone; C: crustal contamination; W: intra plate enrichment; F: fractional crystallization; TH: tholeiitic; CA: calc-alkaline; SHO: shoshonitic

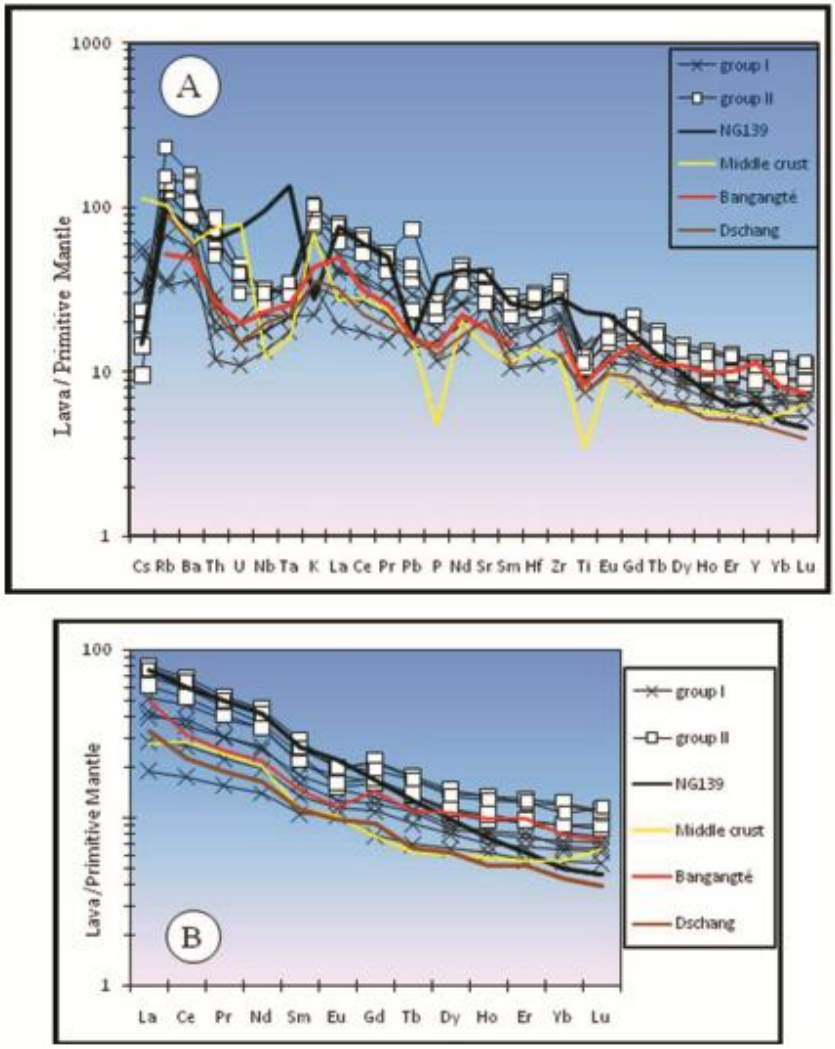

Fig. 11. A: Primitive mantle-normalized [34] multi-element patterns. Data of middle continental crust from [59] and alkali basalt from [12]. B: Chondrite-normalized [34] REE patterns. Bangangté and Manjo data from [29]

5. DISCUSSION

5.1 Dyke Sizes and Implications on Emplacement Process

The numerous doleritic dykes in Mbaoussi area are 3-34 m wide. They are wider than the 0.2 to 1.2 m-wide basaltic dykes of Bangangté, Dschang and Manjo in western Cameroon, 800 km far from Ngaoundéré [29], the 0.5 to 1.5 m wide doleritic dykes of Biden [14] and the 10 to 15 m-wide doleritic dykes of Likok [15]. These one to few kilometer-long dykes may be considered as “giant dykes”, in the sense of [37]. Large sizes imply something about emplacement mechanism. [38] suggested that flows of primitive magma in continental dykes, with widths greater than about 3 m, should be turbulent instead of laminar. Turbulent magma flows feeding Mbaoussi dyke swarm might have favoured some amount of crustal contamination, because flowing magma might have eroded the dyke walls. Occurrence of basement xenoliths evidences possible contamination. On the opposite, laminar flow in the thin dykes of Biden [14], Bangangté, Dschang and Manjo [29] could not have favoured contamination. Individual dyke widths in the swarm indicate that they were related to crustal extension.

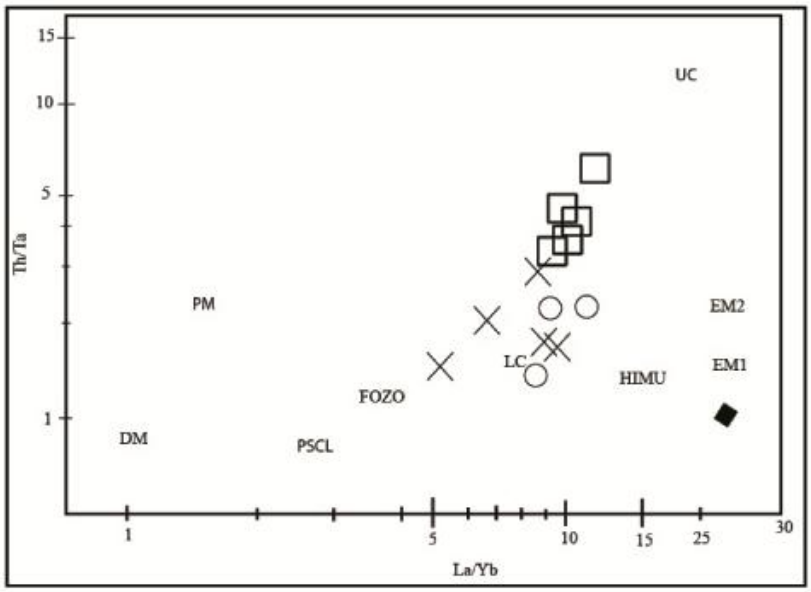

Fig. 12. Th/Ta vs. La/Yb diagram (after [35]. DM: depleted mantle; PM: primitive mantle; PSCL: post-Archean subcontinental lithosphere; LC: lower continental crust: UC, upper continental crust; HIMU: high U/Pb mantle source; EM1 and EM2: enriched mantle sources; FOZO: mantle component (area on the graph beneath and around the word FOZO). Same symbols as Fig. 5

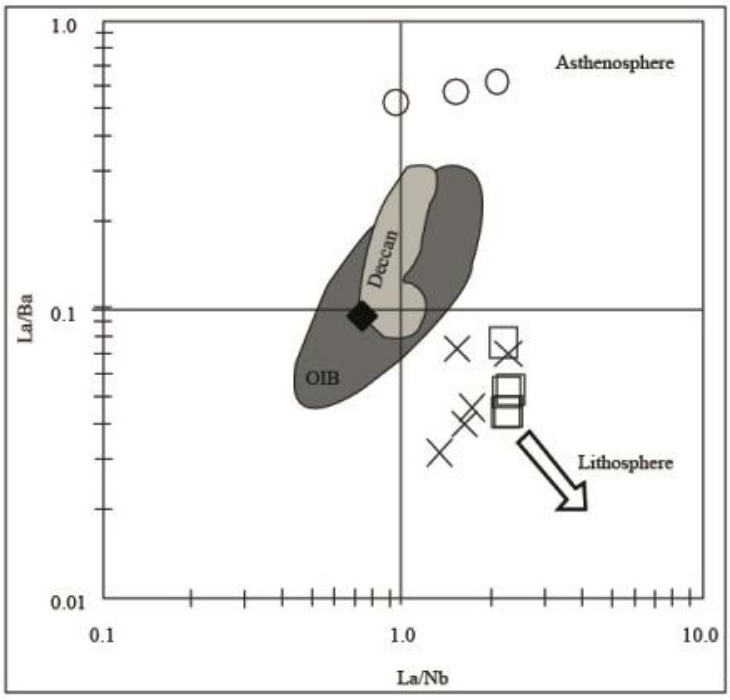

Fig. 13. La/Ba vs. La/Nb diagram (after [36]). Ngaoundéré alkali basalt from [12] and dolerites of Bangante, Dschang and Manjo from [29]. Same symbols as Fig. 5

Field observations show post Pan-African and likely Mesozoic emplacement. Dykes cross-cut basement along N100-120°, and rarely ENE-WSW directions. Fractures have been induced

by Pan-African NW-SE shortening episode, which affected the northern edge of Adamawa plateau [18,39]. Dyke intrusion postdates this tectonic episode and was rather coeval with crustal thinning during or after the main phase of Adamawa horst uplift, as proposed by [7].

5.2 Petrogenesis of Mbaoussi Dyke Swarm

According to total alkalis-silica contents (Fig. 5), Mbaoussi dolerites yield slightly alkaline affinities. CIPW normative variations from silica slightly undersaturated to oversaturated compositions cannot be explained by fractional crystallization of clinopyroxene and plagioclase alone. K, Rb, Ba and Th contents and, to a lesser degree, LREE contents increase from group I to group II dolerites. These values are notably higher than those measured in typical MORB [40]. Group I and group II dolerites are supposed to be co-genetic as shown by relatively constant Zr/Hf (41-47) and Nb/Ta (13-18) ratios and parallel patterns (Fig. 11A and 11B). Thus, both groups define a differentiation series by fractional crystallization.

Fractional crystallization process was probably coupled with slight crustal contamination as indicated by Th/Yb enrichment from group I to group II that might be due to turbulent emplacement (Fig. 10). This has been observed in other continental tholeiites worldwide [41,42,43,44,45,46,47,48]. Low contents of transition elements refer to evolved parental magmas.

Mbaoussi dolerites resemble other dolerites described as continental tholeiites in Cameroon, e.g. at Bangangté [29], Biden [14], and in Nigeria, e.g. at Obudu, in the lower Benue valley [28].

- SiO_2 contents (44.9-53.0 wt%) of Mbaoussi dolerites are in the same range as Obudu and Bangangté continental tholeiites. But they clearly differ from Biden continental tholeiites [14] that have rather high SiO_2 contents (≈ 59 wt%).
- TiO_2 contents (1.5-2.9 wt%) of Mbaoussi dolerites are in the same range as continental tholeiites worldwide [49]. They strongly differ from Ngaoundéré Miocene typical alkaline lava (3-4.6 wt%, [12]).
- Fe_2O_3, MnO, MgO and CaO contents of Mbaoussi dolerites are within the range of nearby dolerites except Biden trachyandesite dolerites characterized by low contents of these elements, and high alkali (Na_2O+K_2O) contents. Mbaoussi dolerites plot in the tholeiitic field that is clearly distinct from the calc-alkaline field, both in FeOt vs. FeOt/MgO diagram (Fig. 7, after [50]) and Alkalis–ΣFeO–MgO triangle (Fig. 8, after [51]).

In primitive Mantle-normalized patterns (Fig. 11A and 11B), all analyzed samples display fractionated REE patterns showing an enrichment of the LREE relative to the MREE and HREE (Fig. 11B) ($(La/Sm)_N$ = 1.8-2.9; $(Ce/Yb)_N$ = 3-7; $(Gd/Yb)_N$ = 1.5-2.0) suggesting garnet in the residue. Lacking Eu anomalies in group I and slightly negative Eu anomalies in group II evidence increasing involvement of plagioclase in fractional crystallization process. Multi-element normalized diagrams (Fig. 11A) illustrate Rb, Ba and K positive anomalies and Nb, Ta, P and Ti pronounced negative anomalies, which may suggest involvement of a subducted slab component in the mantle source [52].

5.3 Mantle Source

Source characteristics of Mbaoussi dolerites are assessed using element-element ratios and trace element patterns as they are particularly characteristic of different magma sources [53] [54] as they are insensitive to magmatic processes in basaltic system [35]. According to [44], incompatible trace element enrichment of continental tholeiite may result from partial melting of the following mantle sources: (1) sub-continental lithospheric mantle (SCLM) (2) depleted asthenosphere and (3) enriched asthenosphere. In the Th/Ta vs. La/Yb diagram proposed by [35], Mbaoussi dolerites exhibit a linear array from FOZO and lower crust (LC) end-members toward upper crust (UC) (Fig. 12). Such array may be due to mixing processes between depleted or primitive mantle end-member and another end-member with high Th/Ta and La/Yb ratios [35]. Partial melting of sub-continental lithosphere and progressive assimilation of continental crust can produce such array. A large amount of heat is required, as noticed by [55] in the case of French Guyana doleritic dykes. Mbaoussi dykes could equally come from a FOZO component somewhat contaminated by Nb-Ta-depleted continental crust.

$(La/Yb)_N$ ratios (values of [34], respectively La = 0.237 and Yb = 0.161 ppm) are commonly used

to discriminate garnet and spinel-rich mantle sources: ratios < 5 identify spinel-bearing mantle, whereas ratios > 5 identify garnet-bearing mantle. Two mantle sources are evidenced: samples D11 and MB3C have fairly low REE contents and $(La/Yb)_N$ ratios of 4.4 and 3.5 respectively. The other samples have higher REE contents and $(La/Yb)_N$ ratios ranging from 5.9 in D2 sample to 7.8 in D12 sample.

Y/Nb ratios, close to 2, seem to typify continental tholeiite. Nb negative anomaly (Fig. 11) could evidence amphibole-bearing metasomatized mantle [56]. However, such a source is not clearly shown in normalized HREE patterns. Indeed, northward to northwestward subduction beneath the Adamawa-Yadé Domain (northern Cameroon–southeastern Chad) occurred between 800 and 630 Ma [57,58] during the Pan-African orogeny and earlier [20]. Mbaoussi dolerites may have been generated from partial melting of spinel-garnet lherzolite mantle enriched in highly incompatible trace elements, yet depleted in Nb and Ta by subduction-derived fluid metasomatism. Magmas en route to the surface, evolving through fractional crystallization, would have assimilated a portion of continental crust, i.e. through AFC (Assimilation and Fractional Crystallization, Fig. 14) processes. With higher contents of incompatible and LREE elements, group II dolerites resulted from group I through progressive crystallization of its constitutive mineral phases.

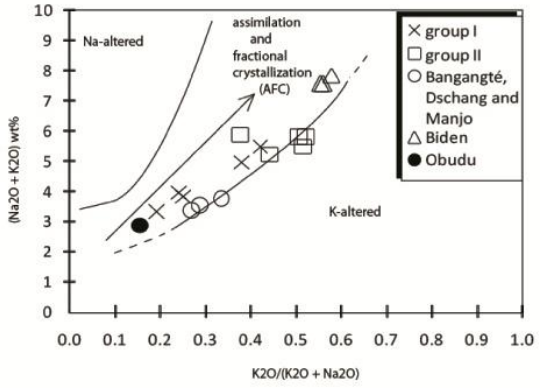

Fig. 14. (Na_2O +K_2O) wt% vs. $K_2O/(K_2O+Na_2O)$ diagram (after [60]). Same symbols as Fig. 5

6. CONCLUSION

Recently discovered dolerite dykes at Mbaoussi in Adamawa plateau are basalt, trachybasalt and basaltic trachyandesite. They reveal some features intermediate between alkaline rocks and continental tholeiites. Original magmas have undergone turbulent flow during their ascent in post Pan-African times. Reworking of Pan-African fault network played an important role. Mbaoussi dolerites have been generated from partial melting of spinel-garnet lherzolite mantle enriched in incompatible trace and LREE elements and depleted in Nb and Ta by fluid metasomatism during earlier subduction. Mbaoussi dolerites comprise two cogenetic groups and constitute a series evolving by fractional crystallization with some contribution of the continental crust.

Authors greatly thank the “Agence Universitaire de la Francophonie (AUF)” through the BAGL (Bureau Afrique Centrale et des Grands Lacs), for financial support of ‘’Le Projet de soutien aux équipes de recherche 2012/2013_No 51110SU201" in all aspects (from field works to laboratory analyses). OFK and AMF spent 3 months in 2013 and AMF spent 2 supplementary months in 2015 as in 2016 at the “Geosciences (GEOPS) laboratory, UMR CNRS 8148” of the University Paris-Sud, Orsay, France. B. Bonin is thanked for fruitful discussions.

COMPETING INTERESTS

Authors have declared that no competing interests exist.

REFERENCES

1. Moreau C, Regnoult JM, Déruelle B, Robineau B. A new tectonic model for the Cameroun line, Central Africa. Tectonophysics. 1987;139:317-334.
2. Dorbath L, Dorbath C, Stuart GW, Fairhead JD. Structure de la croûte sous le plateau de l’Adamaoua (Cameroun). Comptes Rendus de l'Académie des Sciences, Paris. 1984;298:539-542.
3. Browne SE, Fairhead JD. Gravity study of the Central African rift system: A model of continental disruption 1. The Ngaoundéré and Abu Gabra rifts. In: Morgan P & Baker BH, Eds., Processes of planetary rifting. Tectonophysics. 1983;94:187-203.
4. Stuart GW, Fairhead JD, Dorbath L, Dorbath C. A seismic refraction study of the crustal structure associated with the Adamawa Plateau and Garoua Rift, Cameroon, West Africa. Geophysical

Journal of the Royal Astronomical Society. 1985;81:1-12.

5. Fairhead JD, Okereke CS. Depths to major density contrasts beneath the West African rift system in Nigeria and Cameroon based on the spectral analysis of gravity data. Journal of African Earth Sciences. 1988;7:769-777.
6. Poudjom Djomani YH, Diament M, Albouy Y. Mechanical behaviour of the lithosphere beneath the Adamawa Uplift (Cameroon, West Africa) based on gravity data. Journal of African Earth Sciences. 1992;15(1):81-90.
7. Poudjom Djomani YH, Diament M, Wilson M. Lithospheric structure across the Adamawa plateau (Cameroon) from gravity studies. Tectonophysics. 1997;273:317-327.
8. Nnange JM, Ngako V, Fairhead JD, Ebinger CJ. Depths to density discontinuities beneath the Adamawa Plateau region, Central Africa, from spectral analyses of new and existing gravity data. Journal of African Earth Sciences. 2000;30(4):887-901.
9. Nnange JM, Poudjom Djomani YH, Fairhead JD, Ebinger C. Determination of the isostatic compensation mechanism of the region of the Adamawa dome, West Central Africa using the admittance technique of gravity data. African Journal of Science and Technology. 2001;1(1):29-35.
10. Okereke CS. Contrasting modes of rifting: The Benue trough and the Cameroon volcanic line, West Africa. Tectonophysics. 1988;7:775-784.
11. Ambeh WB, Fairhead JD, Francis DJ, Nnange JM, Djallo S. Seismicity of the Mount Cameroon region West Africa. Journal African Earth Sciences. 1989;5(9): 1-7.
12. Nkouandou OF, Ngounouno I, Déruelle B, Ohnenstetter D, Montigny R, Demaiffe D. Petrology of the Mio–Pliocene volcanism to the North and East of Ngaoundéré (Adamawa, Cameroon). Comptes Rendus Geoscience. 2008;340:28-37.
13. Fagny AM, Nkouandou OF, Déruelle B, Ngounouno I. Revised petrology and new chronological data on the peralkaline felsic lavas of Ngaoundéré volcanism (Adamawa plateau, Cameroon, Central Africa): Evidence of open-system magmatic processes. Analele Stiintifice ale Universitatii “Al. I. Cuza” din Iasi Seria Geologie. 2012;58(2):5-22.
14. Vicat JP, Ngounouno I, Pouclet A. Existence de dykes doléritiques anciens à composition de tholéiites continentales au sein de la province alcaline de la ligne du Cameroun. Implication sur le contexte géodynamique. Comptes Rendus de l’Académie des Sciences, Paris. IIA. 2001;332(4):243-249.
15. Nkouandou OF, Fagny AM, Iancu GO, Bardintzeff JM. Petrology and geochemistry of doleritic dyke of Likok (Cameroon, Central Africa). Carpathian Journal of Earth and Environmental Sciences. 2015;10(1):121-132.
16. Ashwal LD, Burke K. African lithospheric structure, volcanism, and topography. Earth and Planetary Science Letters. 1989;96:8-14.
17. Fairhead JD. Mesozoic plate tectonic reconstructions of the central South Atlantic Ocean – The role of the West and Central African Rift system in Nigeria and Cameroon and its tectonic interpretation. Tectonophysics. 1988;143:141-159.
18. Ngangom E. Étude tectonique du fossé Crétacé de la Mbéré et du Djérem, Sud-Adamawa, Cameroun. Bull. Centres de Recherches Exploration-Production, Elf-Aquitaine. 1983;7:339-347.
19. Toteu SF, Penaye J, Poudjom Djomani Y. Geodynamic evolution of the Pan-African belt in Central Africa with special reference to Cameroon. Canadian Journal of Earth Sciences. 2004;41(1):73-85.
20. Tchameni R, Pouclet A, Penaye J, Ganwa AA, Toteu SF. Petrography and geochemistry of the Ngaoundéré Pan-African granitoids in central north Cameroon: Implications for their sources and geological setting. Journal of African Earth Sciences. 2006;44:511-529.
21. White JR, Chappell BW. Ultrametamorphism and granitoids genesis. Tectonophysics. 1977;43:7-22.
22. Dorbath C, Dorbath L, Fairhead JD, Stuart GW. A teleseismic delay time study across the Central African Shear Zone in the Adamawa region of Cameroon, West Africa. Geophysical Journal of the Royal Astronomical Society. 1986;86:751-766.
23. Gill R. Igneous rocks and processes: A practical guide. Wiley-Blackwell, Chichester, UK. 2010;440.
24. Le Maitre RW. Igneous Rocks: A classification and glozssary of terms.

Recommendations of the IUGS Sub-Commission on the Systematics of Igneous Rocks, 2nd edition. Cambridge University Press, Cambridge; 2002.
25. Miyashiro A. Nature of alkalic volcanic rock series. Contributions to Mineralogy and Petrology. 1978;66:91-104.
26. Floyd PA, Winchester JA. Magma type and tectonic setting discrimination using immobile elements. Earth and Planetary Science Letters. 1975;27(2):211-218.
27. Wilkinson JFG, Le Maitre RW. Upper mantle amphiboles and micas and TiO_2, K_2O and P_2O_5 abundances and 100Mg/(Mg+Fe^{2+}) ratios of common basalts and andesites: Implications for modal mantle metasomatism and undepleted mantle compositions. Journal of Petrology. 1987;28:37-73.
28. Ekwueme BN. Basaltic magmatism related to the early stages of rifting along the Benue Trough: The Obudu dolerites of south-east Nigeria. Geological Journal. 1994;29(3):269-276.
29. Tchouankoue JP, Wambo NAS, Kagou Dongmo A, Wörner G. Petrology, geochemistry, and geodynamic implications of basaltic dyke swarms from the Southern continental part of the Cameroon Volcanic Line, Central Africa. The Open Geology Journal. 2012;6:72-84.
30. Thompson RN, Dickin AP, Gibson IL, Morrison MA. Elemental fingerprints of isotopic contamination of hebridean Palaeocene mantle-derived magmas by Archaean sial. Contributions to Mineralogy and Petrology. 1982;79(2):159-168.
31. Sivell WJ. Geochemistry of metatholeiites from the harts range, Central Australia: Implications for mantle source heterogeneity in a Proterozoic mobile belt. Precambrian Research. 1988;40-41:261-275.
32. Meschede M. A method of discriminating between different types of mid-ocean ridge basalts and continental tholeiites with the Nb-Zr-Y diagram. Chemical Geology. 1986;56(3-4):207-218.
33. Pearce JA. Trace elements characteristics of lavas from destructive plate boundaries. J. Wiley and Sons, Chichester. In: Thorpe RS, Ed., Andesite. 1982;525-548.
34. McDonough WF, Sun SS. The composition of the earth. Chemical Geology. 1995;120:223-253.
35. Condie KC. Sources of Proterozoic mafic dyke swarms: Constraints from Th/Ta and La/Yb ratios. Precambrian Research. 1997;81(1-2):3-14.
36. Saunders AD, Storey M, Kent RW, Norry MJ. Consequences of plume-lithosphere interactions. In: Storey BC, Alabaster T, Pankhurst RJ, Eds., Magmatism and the Causes of Continental Break-up. Geological Society of London Special Publication. 1992;68:41-60.
37. Bryan SE, Ernst RE. Revised definition of large igneous provinces (LIPs). Earth-Science Reviews. 2008;86:175-202.
38. Campbell IH. The difference between oceanic and continental tholeiites: A fluid dynamic explanation. Contributions to Mineralogy and Petrology. 1985;91:37-43.
39. Dumont JF. Étude structurale des bordures nord et sud du plateau de l'Adamaoua: Influence du contexte Atlantique. Géodynamique. 1987;2(1):55-68.
40. Holm PE. The geochemical fingerprints of different tectonomagmatic environments using hygromagmatophile element abundances of tholeiitic basalts and basaltic andesites. Chemical Geology. 1985;51:303-323.
41. Dupuy C, Dostal J. Trace element geochemistry of some continental tholeiites. Earth and Planetary Science Letters. 1984;67(1):61-69.
42. Marsh JS. Geochemical constraints on coupled assimilation and fractional crystallization involving upper crustal compositions and continental tholeiitic magma. Earth and Planetary Science Letters. 1989;92:70-80.
43. Valbracht PJ, Helmers H, Beunk FF. Early proterozoic continental tholeiites from western Bergslagen, Central Sweden, I. Petrology, geochemical petrogenesis and geotectonic setting. Precambrian Research. 1991;52:187-214.
44. Tembo F, Kampunzu AB, Porada H. Tholeiitic magmatism associated with continental rifting in the Lufilian fold belt of Zambia. Journal of African Earth Sciences. 1999;28(2):403-425.
45. Cadman AC, Tarney J, Bridgewater D, Mengel F, Whitehouse MJ, Windley BF. The petrogenesis of the Kangamiut dyke swarm, W. Greenland. Precambrian Research. 2001;105:183-203.
46. Srivastava RK, Singh RK. Trace element geochemistry and genesis of Precambrian sub-alkaline mafic dikes from the central

Indian craton: Evidence for mantle metasomatism. Journal of Asian Earth Sciences. 2004;23:373-389.
47. Ingle S, Scoates JS, Weis D, Brugmann G, Kent RW. Origin of cretaceous continental tholeiites in southwestern Australia and eastern India: Insights from Hf and Os isotopes. Chemical Geology. 2004;209:83-106.
48. Worthing MA. Petrology and geochronology of a Neoproterozoic dyke swarm from Marbat, South Oman. Journal of African Earth Sciences. 2005;41:248-265.
49. Wayne TJ. Lithophile elements in Huronian low-Ti continental tholeiites from Canada, and evolution of the Precambrian mantle. Earth and Planetary Science Letters. 1987;85:401-415.
50. Miyashiro A. Volcanic rock series in island arcs and active continental margins. American Journal of Science. 1974;274(4): 321-355.
51. Irvine TN, Baragar WRA. A Guide to the chemical classification of the common volcanic rocks. Canadian Journal of Earth Sciences. 1971;8(5):523-548.
52. Sun SS, McDonough WF. Chemical and isotopic systematics of ocean basalt: Implications for mantle composition and processes. In: Saunders AD, Norry MJ, Eds., Magmatism in the ocean basins. Geological Society, London. 1989;313-344.
53. McCulloch MT, Gamble JA. Geochemical and geodynamical constraints on subduction zone magmatism. Earth and Planetary Science Letters. 1991;102:358-374.
54. Carlson RW. Physical and chemical evidence on the cause and source characteristics of flood basalt volcanism. Australian Journal of Earth Sciences. 1991;38(5):525-544.
55. Nomade S, Pouclet A, Chen Y. The French Guyana doleritic dykes: Geochemical evidence of three populations and new data for the Jurassic Central Atlantic Magmatic Province. Journal of Geodynamics. 2002;34:595-614.
56. Vaselli O, Downes H, Thirlwall MF, Vannucci R, Coradossi N. Spinel-peridotite xenoliths from Kapfenstein (Graz Basin, Eastern Austria): A geochemical and petrological study. Mineralogy and Petrology. 1996;57:23-50.
57. Njonfang E, Ngako V, Kwekam M, Affaton P. Les orthogneiss calco-alcalins de Foumban–Bankim: Témoins d'une zone interne de marge active panafricaine en cisaillement. Comptes Rendus Geoscience. 2006;338:606-616.
58. Toteu SF. Geochemical characterization of the main petrographical and structural units of Northern Cameroon: Implications for Pan-African evolution. Journal of African Earth Sciences. 1990;10(4):615-624.
59. Rudnick RL, Fountain DM. Nature and composition of the continental crust: A lower crustal perspective. Reviews of Geophysics. 1995;33(3):267-309.
60. Hughes CJ. Spilites, keratophyres and the igneous spectrum. Geological Magazine. 1973;109:513-527.

Peer-review history:
The peer review history for this paper can be accessed here:
http://sciencedomain.org/review-history/16647